



**Research on Electrical Discharge
Machining of Polycrystalline
Diamond**

A thesis submitted in fulfilment of the requirements for the degree of Doctor of Philosophy

Mohammad Zulafif Rahim

M. Eng. (Advanced Manufacturing Technology)

B. Eng. (Hons) (Mechanical-Manufacturing)

School of Aerospace Mechanical and Manufacturing Engineering

College of Science Engineering and Health

RMIT University

June 2015

Abstract

The non-contact process of Electrical Discharge Machining (EDM) eliminates cutting forces, and is regarded as the most effective process to machine polycrystalline diamond (PCD). However, the EDM plasma temperature of up to 12000K in the EDM process will cause damage to the machined surface. With emphasis on the cutting tool product, this study focuses on the analysis of the PCD surface damage caused by the Electrical Discharge Grinding (EDG) process and its optimization strategies. In addition to the graphitization and residual stress, several issues that assumed to be thermal damage indications caused by the process are highlighted. These include the formation of porous surfaces, cutting edge undercuts and some cosmetic aspects at the WC-PCD interface. It was found that the high temperature generated during erosion resulted in the partial conversion of diamond to graphite phase under the surface. Higher finishing in-feed proved to produce better surface quality by means of lower surface graphitization and lower tensile residual stress. The comprehensive discussion undertaken includes the theoretical modelling of the process, together with the validated results. The structural difference and residual stress between PCD manufactured with EDG and conventional grinding have been compared. Performance tests have also been conducted at the end of the methodology to evaluate and validate the models.

Table of Contents

Declaration	ii
Abstract	iv
Acknowledgements	v
Publications	vi
List of Figures	xii
List of Tables.....	xvii
Symbols.....	xviii
Chapter 1 Introduction	1
1.1. Research Background.....	1
1.2. Objectives and Research Questions.....	3
1.3. Scope of the Investigation	5
1.4. Challenges in PCD Tools Fabrication	6
1.5. Research Methodology	8
Chapter 2 Literature Review	10
2.1. Introduction	10
2.2. PCD EDM Process	11
2.2.1. EDM Polarity.....	12
2.2.2. Material Removal Rate	15
2.2.3. Surface Roughness and Morphology.....	17
2.2.4. Challenges on Cutting of Laminar Discs.....	21
2.2.5. Heat Affected Zone (HAZ).....	22
2.2.6. Material Phase Transformation.....	25
2.3. Conclusion.....	28
Chapter 3 Experiment Procedure and Method of Analysis.....	29
3.1. Introduction	29
3.2. Electrical Discharge Grinding Process	29
3.3. Raman analysis	33
3.4. XRD Analysis.....	37
3.5. XRD vs. Raman analysis in Residual Stress and Graphitization Analysis .	39
3.6. Conclusion.....	41

Chapter 4 Investigation on the Effect of Electrode Polarity	42
4.1. Introduction	42
4.2. Experimental Procedure	43
4.3. Result and Discussion.....	48
4.3.1. Morphological Analysis.....	48
4.3.2. Material Removal Rate	55
4.4. Conclusion.....	62
Chapter 5 Investigation on the Effect of Wheel Rotation Direction	64
5.1. Introduction	64
5.2. Equipment and Methodology	66
5.3. Results and Discussion	70
5.4. Conclusion.....	81
Chapter 6 Investigation on the Effect of Machining Parameters and Its Theoretical Modelling	83
6.1. Introduction	83
6.2. Equipment and Methodology	85
6.3. Results and Discussion	87
6.3.1. Effect of Roughing Process	87
6.3.2. Theoretical Model.....	93
6.3.3. Effect of Finishing Operation	105
6.3.4. Single Discharge Test	111
6.4. Conclusion.....	114
Chapter 7 Tool Quality Investigation and Performance Analysis	116
7.1. Introduction	116
7.2. Methodology.....	118
7.2.1. Conventional Grinding Parameter Selection	118
7.2.2. EDG Machining Parameters Selection	120
7.2.3. Morphological, Structural Quality, and Residual Stress Analysis.....	121
7.2.4. Performance Analysis	122
7.3. Results and Discussion	123
7.3.1. Morphological Analysis.....	123
7.3.2. Residual Stress and Graphitization Analysis	127
7.3.3. Performance Test	133

7.4. Conclusion.....	141
Chapter 8 Tool Quality Assessment and Validation	143
8.1. Introduction	143
8.2. Methodology.....	144
8.3. Result and Discussion.....	146
8.4. Conclusion.....	154
Chapter 9 Summary.....	155
9.1. Summary.....	155
9.2. Future Work.....	159
9.2.1. Investigation on Material Removal Rate	159
9.2.2. Mathematical modelling of thermal residual stress	159
9.2.3. An extensive investigation on PCD tool invisible quality	160
References	161

List of Figures

Figure 1: Example of special geometry drill-bit commercially available in machining of fibre reinforced plastic material [7]	2
Figure 2: Weekly tool usage in Boeing Aerostructures Australia.....	4
Figure 3: PCD tool.	6
Figure 4: Edge undercut	7
Figure 5: Research methodology	8
Figure 6: Illustration of the process flow	8
Figure 7: Graphite Coating Method	12
Figure 8: Comparison of electrode shape obtained by SEM after different polarity machining. (a) Initial shape of electrode (before machining) (b) Electrode after the positive polarity erosion (positive polarity of the tool electrode) (c) Electrode shape after negative polarity erosion (negative polarity of the tool electrode)[6]	14
Figure 9: MRR optimization strategies	16
Figure 10:EDMed surfaces of boron doped PCD sample[53]	19
Figure 11: Void due to selective erosion [59].....	21
Figure 12: Element Mapping of (a) C, (b) Co, (c) Ta and (d) W [62]	22
Figure 13: Heat affected zone of EDMed surface [58]	23
Figure 14: SEM image of PCD (a) after EDM (b) after LWJ [65, 66]	24
Figure 15: PCD structure [21].....	25
Figure 16: Carbon phase diagram [10].....	26
Figure 17: Distribution of chemical elements close to the EDMed edge[59].....	27
Figure 18:RX7 EDG machine.....	30
Figure 19: Schematic of the EDG process	30
Figure 20: Discharge phases in EDM [87].....	31
Figure 21: EDG equipment (a) Pulse generator (b) Data acquisition system	33
Figure 22: Raman spectra result on composition of electrode (A) before EDM, (B) after EDM [6].....	35
Figure 23: SEM image of 10 μ m synthetic diamond particles.	36
Figure 24:Raman spectra of the unstressed diamond grains	36
Figure 25: Experimental setup and procedure	46
Figure 26: Block diagram of the EDM gap control system	47

Figure 27: Surface produced by finishing operation. (a) Negative polarity.	48
Figure 28: Close up view of the surfaces produced. (a) Negative polarity.	49
Figure 29: EDX surface mapping	49
Figure 30: Elemental composition (a) Negative polarity, (b) Positive polarity	51
Figure 31: XRD analysis of the surface eroded with different polarities (a) Negative polarity, (b) Positive polarity	52
Figure 32: Raman Analysis: (a) Raman shift value, (b) FWHM analysis of the Raman spectrum.....	54
Figure 33: Illustration of the black layer assisted erosion theory	55
Figure 34: Material erosion rate of different PCD types (positive polarity).....	56
Figure 35: Material erosion rate of different PCD types (negative polarity).....	57
Figure 36: Residue surface left by the roughing surface: (a) SEM image (CTB010), (b) Surface profile (CTX002), (c) Surface profile (CTB010), (d) Surface profile (CTM302)	58
Figure 37: Non-linear regression line fitting.....	59
Figure 38: The images of deposited material on the eroded surface of CTM302 PCD (obtained by the optical microscope with 100x magnification lens): (a) After 10 μ m finishing in-feed; (b) After 20 μ m finishing in-feed; (c) After 30 μ m finishing in- feed; (d) After 40 μ m finishing in-feed.....	60
Figure 39: SEM image of the black layer	60
Figure 40: Elemental composition of the black layer (The image taken is perpendicular from the eroded surface)	61
Figure 41: MRR versus wheel speed	67
Figure 42: Experimental methodology (wheel direction): (a) Counter-clockwise (ccw), (b) Clockwise (cw), (c) Actual EDG process	68
Figure 43: Specimen: (a) Description of the specimen; (b) PCD strip (before erosion); (c) Specimen with 50° apex angle (after erosion).....	69
Figure 44: Measurement method: (a) Alicona optical measuring device used in the experiment; (b) 3D image of the PCD edge obtained by Alicona; (c) Position of extracted profile paths for tool sharpness measurement	70
Figure 45: Definition of sharpness parameter.....	70
Figure 46: Comparison between Sa and Sy obtained by two different methods, which are WC to PCD (ccw wheel rotation) and PCD to WC (cw wheel rotation).....	71

Figure 47: Effect of wheel rotation on the edge radius and symmetry (1=symmetry)	72
Figure 48: Schematic of fluid flow under a moving plate	73
Figure 49: SEM image of the eroded surface using different wheel rotation direction: (a) ccw wheel rotation direction (300x magnification); (b) cw wheel direction (300x magnification); (c) ccw wheel direction (2000x magnifications); (d) cw wheel direction (2000x magnification); (e) Illustration of the spark concentration phenomenon	74
Figure 50: Undercut formed due to continuous uneven sparking on the PCD edge (image taken from the eroded surface)	75
Figure 51: Extraction position for the edge roughness measurement	75
Figure 52: The roughness (Ra) of PCD edges measured by Alicona device	76
Figure 53: SEM image of the cutting edge produced (images taken from the polished surface): (a) 90 degree apex angle with cw wheel direction; (b) 70 degree apex angle with cw wheel direction; (c) 50 degree apex angle with cw wheel direction; (d) 90 degree apex angle with ccw wheel direction; (e) 70 degree apex angle with ccw wheel direction; (e) 50 degree apex angle with ccw wheel direction	77
Figure 54: Results of Raman analysis	78
Figure 55: Effect of higher wheel speed	78
Figure 56: 3D images of the eroded surface: (a) cw wheel direction; (b) ccw wheel direction	79
Figure 57: Cross-section profile of the surface: (a) cw wheel direction; (b) ccw wheel direction	79
Figure 58: Notch size	80
Figure 59: Illustration of the electrolyte flow and debris accumulation: (a) cw wheel direction; (b) ccw wheel direction; (c) Actual image of the notch	81
Figure 60: Three stages of the residual stress formation in tool production	83
Figure 61: SEM images of the PCD after roughing (modified zone was clearly observed on the 12A PCD sample)	88
Figure 62: SEM and Backscatter Image of modified zone	89
Figure 63: Raman analysis	89
Figure 64: SEM images (left) and backscatter images (right) of the eroded PCD by roughing	92

Figure 65: Inspection location (the collected debris was deposited on the carbon tape)	92
Figure 66: Thermal stress components considered in the model (r = position where the stress is estimated, a = diamond grain radius, σ = stress component for tangential, t and radial, r direction) [86]	93
Figure 67: Temperature-dependent properties of diamond.....	97
Figure 68: Current, voltage, spark radius, and heat flux value used in the model	99
Figure 69: Scheme for the boundary conditions	100
Figure 70: Temperature-dependent properties calculated.....	102
Figure 71: Temperature-stress relationship for different PCD	104
Figure 72: Diamond breakage mechanism.....	105
Figure 73: Eroded surface by the finishing operation.....	106
Figure 74: Raman D-value (a) CTX002 (b) CTB010 (c) CTM302.....	108
Figure 75: D/G ratio (a) CTX002 (b) CTB010 (c) CTM302.....	110
Figure 76: A comparison of graphitization degree of three different PCD.....	111
Figure 77: Current, voltage, spark radius, and heat flux value used in the model ...	112
Figure 78: The profile of two craters (a) and (b) on the PCD surface	113
Figure 79: ANSYS simulation result	114
Figure 80: Grinding process of PCD: (a) Machine setup; (b) PCD insert holder ...	119
Figure 81: EDG process of PCD: (a) Machine setup; (b) PCD insert holder	120
Figure 82: Experimental setup	123
Figure 83: Surface roughness: (a) CTX002 ground surface; (b) CTB010 ground surface; (c) CTX302 ground surface; (d) Eroded surface.....	124
Figure 84: SEM Images of CTB010: (a) Eroded PCD; (b) Ground PCD.....	125
Figure 85: Cutting edge radius: (a) CTX002 ground surface; (b) CTB010 ground surface; (c) CTX302 ground surface; (d) Eroded surface.....	126
Figure 86: SEM image of the cutting edge CTB010 prepared by different methods: (a) EDG erosion; (b) Conventionally ground with 10m/s wheel velocity 5 μ m in-feed	127
Figure 87: Raman value of the Ground PCD: (a) CTX002 ground surface; (b) CTB010 ground surface; (c) CTX302 ground surface; (d) Eroded surface.....	129
Figure 88: Raman spectra of ground polycrystalline diamond	131
Figure 89: Raman spectra of eroded polycrystalline diamond.....	132

Figure 90: 3D images of the worn cutting tools, grooves prepared by specific PCD tools insert and their cross-sectional profile: (a) Eroded CTB010 (10 μ m finishing in-feed); (b) Eroded CTB010 (40 μ m finishing in-feed); (c) Ground CTB010 (10m/s machining velocity, 0.2mm/min feed rate)	134
Figure 91: Wear mode of the cutting tools (CTX002): (a) Eroded (10 μ m finishing in-feed); (b) Eroded (40 μ m finishing in-feed); (c) Ground.....	135
Figure 92: Wear mode of the cutting tools (CTB010): (a) Eroded (10 μ m finishing in-feed); (b) Eroded (40 μ m finishing in-feed); (c) Ground.....	136
Figure 93: Wear mode of the cutting tools: (CTM302) (a) Eroded (10 μ m finishing in-feed); (b) Eroded (40 μ m finishing in-feed); (c) Ground	137
Figure 94: EDX spectrum of point A.....	138
Figure 95: Relationship between sharpness and cutting force: (a) Used cutting edge; (b) z-direction cutting force value.....	139
Figure 96: Cutting tip shortening and their effect on the cutting force.....	139
Figure 97: Cutting force produced by ground PCD	140
Figure 98: Experimental setup for the turning test.....	145
Figure 99: Raman analysis of the PCD surface	146
Figure 100: Flank wear after each stage of turning experiment.....	147
Figure 101: PCD tools after 30 seconds of the turning process: (a) 3-stage PCD; (b) 2-stage PCD; (c) Ground PCD	150
Figure 102: PCD tools after 10 minutes of the turning process: (a) 3-stage PCD; (b) 2-stage PCD; (c) Ground PCD	151
Figure 103: PCD nose wear and their effect to the chip formation after 10 minutes of the turning process: (a) 3-stage eroded PCD; (b) 2-stage eroded PCD; (c) Ground PCD	152
Figure 104: Work piece surface after 1 minute machining: (a) 3-stage eroded PCD; (b) 2-stage eroded PCD; (c) Ground PCD	153
Figure 105: Work piece surface after 10 minute's machining: (a) 3-stage eroded PCD; (b) 2-stage eroded PCD; (c) Ground PCD	153

List of Tables

Table 1: Erosion resistance index (ERI) of materials [6].....	15
Table 2: Comparison between PCD and CVDITE CDE material	18
Table 3: Peak band centre for the Raman analysis as carbon lattice structure identification [6, 83, 90].....	34
Table 4: Overview of selected literatures.....	39
Table 5: Finishing strategies	43
Table 6: Properties of PCD [98-100]	44
Table 7: EDG machining parameters.....	44
Table 8: EDG parameters for specimen preparation.....	66
Table 9: EDG parameters for the roughing experiment.....	86
Table 10: Properties of PCD [98-100]	86
Table 11: EDG parameters for the finishing experiment.....	87
Table 12: Properties of diamond and cobalt	96
Table 13: Comparative study between the theoretical values obtained from the physical model and the real value	109
Table 14: Properties of PCD [98-100]	118
Table 15: EDG machining parameters.....	121
Table 16: Properties of Ti-6Al-4V used.....	144
Table 17: Chemical composition of the work piece.....	144
Table 18: 3-stage erosion parameters.....	145

Symbols

A	cross sectional area	(mm ²)
a	diamond grain radius	(μm)
C	specific heat of material	(J/kgK)
C_m	erosion resistance index	(10 ¹² J ² / m s kg)
c_c	heat capacitance for cobalt	(J/kgK)
c_d	heat capacitance for diamond	(J/kgK)
d	lattice spacing	(nm)
E	modulus of elasticity	(N/m ²)
E_d	discharge energy	(J)
ε	strain	
f_c	cobalt fraction	
f_d	diamond fraction	
h	sparking gap distance	(μm)
i	current	(A)
K	thermal conductivity	(W/mK)
k_d	thermal conductivity of diamond	(W/mK)
k_c	thermal conductivity of cobalt	(W/mK)
\dot{m}	volume erosion rate	(mm ³ /s)
q	heat flux	(J/s)
r	position where the stress value is determined	(μm)
r_p	plasma radius	(μm)
\dot{s}	feed rate	(mm/s)
T	temperature	(K)
T_m	melting point	(K)
t	pulse duration	(μs)
U	voltage	(V)
u	thermal displacement	(μm)
V	viscosity	(kg/ms)

ν	Poisson's ratio	
ν_r	unstressed Raman value	(cm^{-1})
ν_s	Raman shift value	(cm^{-1})
χ	coefficient of stress-induced frequency shift	(N/m^2)
α	coefficient of thermal expansion	(K^{-1})
θ	temperature difference	(K)
θ_c	X-ray diffraction angle	(degree, $^\circ$)
λ	elastic modulus	
λ_c	X-ray wavelength	(nm)
μ	shear modulus	
σ	tensile residual stress	(N/m^2)
σ_t	tangential stress	(N/m^2)
σ_r	radial stress	(N/m^2)
Ψ	X-ray diffraction tilt angle	(degree, $^\circ$)

Chapter 1 Introduction

1.1. Research Background

Known as a hard and brittle material, polycrystalline diamond (PCD) is produced from diamond particles that are sintered together under high temperature and high pressure conditions (at temperatures of 1670K to 1770K and pressures of 5GPa to 6GPa) in the presence of a catalytic metal [1-4]. PCD is becoming popular because of its excellent physical characteristics. It has been applied widely in die and cutting tool applications due to the high hardness, good thermal conductivity, high strength, and chemical resistance to most corrosive environments [5, 6]. Until 1996, applications of PCD tools were monopolized by the automotive sector due to the limitations of the process, which is efficient only in forming simple shapes [1]. Conventionally abrasive grinding processes have been established as the fabricating method for PCD cutting tools. Although better surface roughness can be obtained by conventional grinding, low grinding efficiency and large grinding forces induced during the process are inherent problems that limit the wide application of PCD tools. The non-contact process of Electric Discharge Machining (EDM) eliminates cutting forces, and is regarded as the process that will result in a better application by means of process flexibility with lower production costs [6]. For this reason, nowadays, further investigation on EDM of PCD is becoming extensive, and EDM is expected to be the best strategy in integrating the complicated geometric shape and superior properties of PCD for optimized process characteristics. Figure 1 shows an example of complicated tools shape that demand high process flexibility.

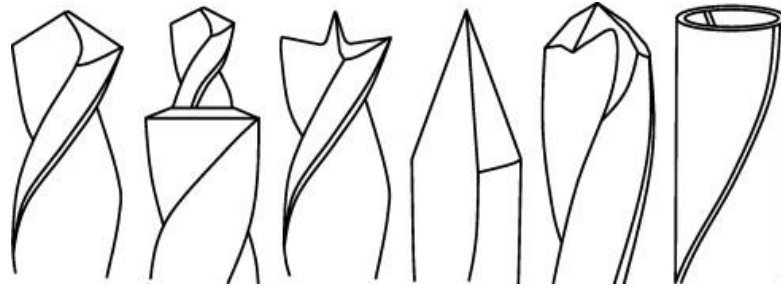


Figure 1: Example of special geometry drill-bit commercially available in machining of fibre reinforced plastic material [7]

However, the EDM plasma with the temperature of up to 12000K in the EDM process will cause damage to the machined surface [1]. Erasmus et al. [8] reported that the PCD material would be subjected to reduction in compression stress when it was repeatedly annealed to about 1070K. This might be due to the graphitization process catalysed by the cobalt (and typically has an onset temperature of around 1020K) [8]. The effect is expected to be more dominant for the EDMed surface, since the temperature is comparatively much higher than the annealing temperature.

The damaged surface or surface integrity associated with the thermal effect include graphitization and residual stress. This surface damage is usually correlated with the zone termed the Heat Affected Zone (HAZ). In order to achieve better performance, surface damage or defects should be controlled. Surface defects will induce stress concentration that is also considered a weak spot for crack propagation. Removing the damaged surface by grinding is not the best solution, especially when the surface geometry is complex.

The available research includes the strategies on how to overcome the major drawback in EDM, which is low production rate, and high surface roughness. However, the PCD industries, especially in cutting tool production, should not only consider the economic aspect, but also need to place emphasis on the quality aspect of the product. The primary concern is that there is insufficient data on the surface quality or surface integrity relating to the application performance of the tools. With

emphasis on the cutting tool product, this study is focused on the analysis of the Polycrystalline Diamond (PCD) surface damage caused in the fabrication process, specifically in the Electrical Discharge Grinding (EDG) process, and its optimization strategies.

1.2. Objectives and Research Questions

Since its development, PCD has been applied in the aerospace, automotive, wood and mining industries as cutting tools due to its outstanding cutting performance. Because of the ultra-hardness and low electric conductivity, PCD tools are very difficult to fabricate. The high costs caused by low machining efficiency have seriously hindered its widespread application in industry.

Although PCD tools are superior in toughness (chipping resistance), a 300% to 500% scatter in tool life has been reported in the automotive industries [9]. Indeed, unexplained breakages of PCD tools used for similar applications are also common [2, 9]. In addition to the direct cost of the tools, indirect costs are caused by the large amount of time needed to replace failed tools and set up new ones on each shift each day, which causes huge losses to the company over the long run. Figure 2 shows an example of weekly tool consumption for the drilling and milling of carbon fibre reinforced plastic (CFRP) components at Boeing Aerostructures Australia (a medium size company at Port Melbourne, Australia). High performance PCD tools with a much longer tool life would have been a perfect solution.

However, there is as yet no theory to explain adequately the relationships between tool life and the modified PCD properties after specific fabrication or machining strategy. Owing to the special structure of PCD, the EDM erosion process is very complex. The machining mechanism is distinctively different from conventional electrical conductive material. Because of the lack of theoretical support on the modified PCD properties after erosion, industry EDG technology has to rely on visible qualities, such as surface finish and geometrical accuracy, in order to define

the quality of the PCD tools. In fact, the author found that the other factors, such as residual stress and graphitization significantly altered the PCD tool life, although similar visible quality is achieved.



Figure 2: Weekly tool usage in Boeing Aerostructures Australia

As an attempt to resolve the issues, the following research objectives are defined:

- a. To develop a new methodology to identify HAZ.
- b. To find the best method to quantify the residual stress on PCD.
- c. To investigate the effects of plasma temperature generated by electrical sparks on PCD tool life.
- d. To optimize the EDG parameters (electrode polarity, wheel rotation direction, pulse on-time, pulse off-time, sparking voltage, and finishing in-feed) to improve PCD tool performance.

The key research questions are:

- a. How to determine the HAZ in PCD?
- b. What are the structural differences between PCD tools manufactured with different EDG processes?
- c. What are the differences in residual stress between PCD tools manufactured with EDG and conventional grinding processes?

- d. What is the relationship between the plasma temperature in the EDG process and PCD tool quality (tool life)?
- e. How will the machining parameters (electrode polarity, wheel rotation direction, pulse on-time, pulse off-time, sparking voltage, and finishing in-feed) affect the wear behaviour of PCD tools?

1.3. Scope of the Investigation

The scope of this study is as follows:

- a. The research includes both theoretical and experimental knowledge analysis.
- b. PCD samples with cobalt binder and different particle sizes will be used in this investigation.
- c. Finishing processes are limited to conventional grinding and EDG.
- d. CNC cutting tests will be conducted to prove and validate theoretical findings.

1.4. Challenges in PCD Tools Fabrication

PCD is commonly produced in a thin layer of 0.5mm to 0.7mm thickness on a supporting layer of tungsten carbide (WC). PCD tools are usually fabricated in three steps:

- a. Cut PCD blanks into small inserts;
- b. Braze the inserts on a carbide substrate;
- c. Machine and sharp the cutting edges into the required dimension and surface finish.

Figure 3 shows an example of PCD tools for the milling process.

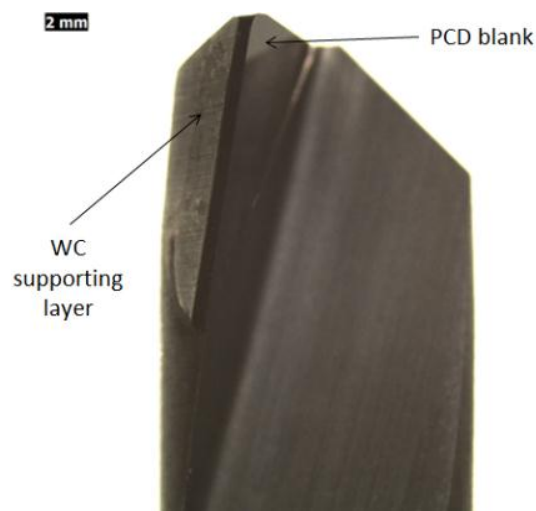


Figure 3: PCD tool.

The research was begun with the observation of the PCD tools' surface quality after erosion. Several issues that were assumed as thermal damage indications caused by the process were highlighted. This included the formation of cutting edge undercut and some cosmetic aspects at the WC-PCD interface. However, whether the phenomena are the real implications of thermal damage was in question. Figure 4 shows the example of edge undercut mentioned. Initially, it was inferred that the formation of edge undercut happened due to the excessive tensile stress generated on the tip. However, the inference was incorrect and the exact reasons have been

reported in this thesis. Since the issue was reported previously but unexplained, the study was regarded as the first that successfully resolved the issue.

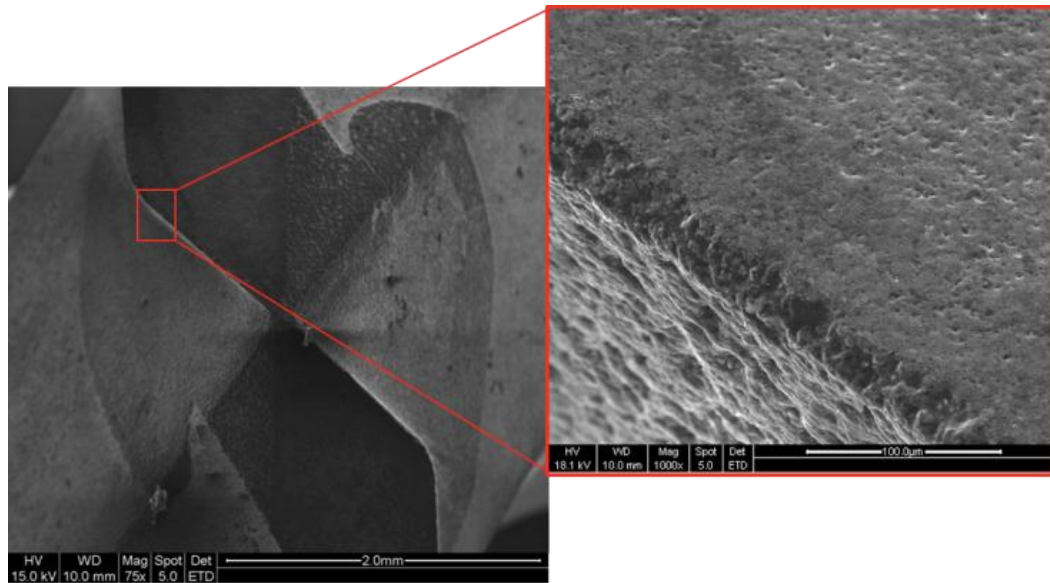


Figure 4: Edge undercut

From the industrial perspective, a notch that appeared on the WC-PCD interface is also considered a temperature-induced defect. Due to the difficult-to-observe PCD thermal damage, the notch appearance is referred to as gauging the damage level. With the bigger notch that appeared after erosion, a bigger thermal impact is predictably performed on the surface during erosion. With this hypothesis, the notch becomes an industrial concern. However, the emergence of this hypothesis became confusing when inconsistent notch width was achieved with similar repetition of the process. Regarding this issue, two possibilities were drawn as follows:

- a. There is an uncontrolled variable that affects the process.
- b. The machine system is unstable, and this then caused inconsistency in energy supplied for the plasma development.

The thermal damage issues are as yet not well understood by the research community. In order to gain better understanding of the PCD thermal damage, a series of scientific investigations on process stability is urgently required. Chapters 4 and 5 discuss the importance of some control factors and the findings related to these issues.

1.5. Research Methodology

The flowchart in Figure 5 shows the methodology of the research.

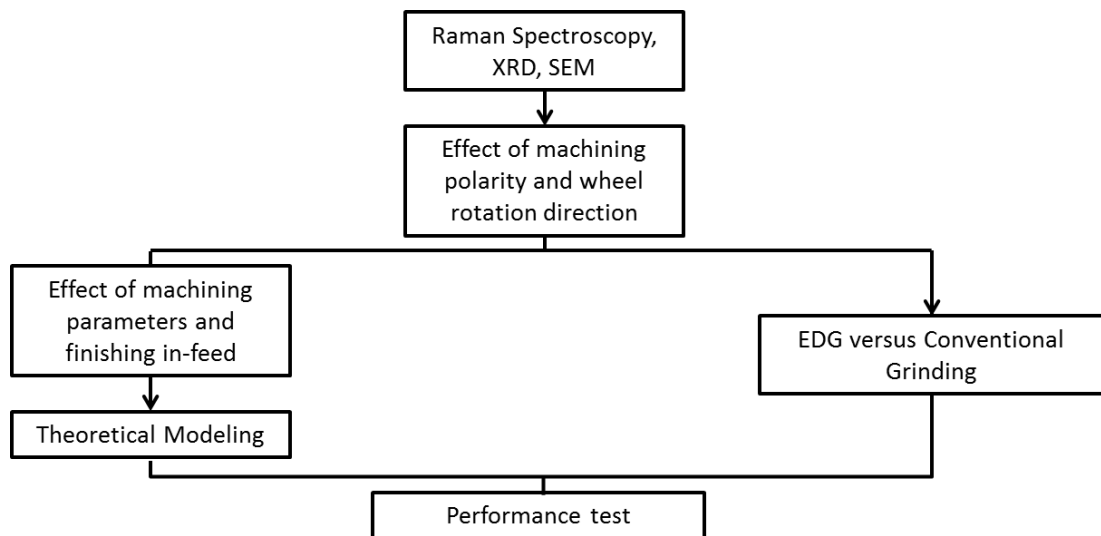


Figure 5: Research methodology

The alteration of residual stress and phase transformation (graphitization) was expected to indicate the HAZ of the PCD due to the erosion process. Metallurgical examination methods, such as optical metallography, Scanning Electron Microscope (SEM), X-ray diffraction (XRD) and Raman spectroscopy, were identified as suitable instruments for the analysis. Through the literature, it was found that the Raman method is the best method for residual analysis determination. The small laser spot size and reasonably small penetration depth were found to provide better measurement accuracy than XRD. This was considered a highly sensible method for being able to detect amorphous carbon structure.

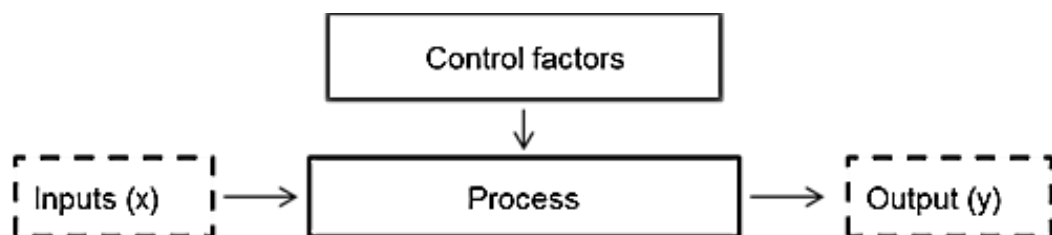


Figure 6: Illustration of the process flow

Determination of the control factors is a vital procedure for ensuring good repeatability of the process and avoiding obstruction or interference of external elements with the results obtained. Focusing on the surface quality and the cutting edge sharpness, the effects of tool polarity and wheel rotation direction were determined. The best strategies were then taken as the standard in the succeeding investigation.

As the next step, the PCD-eroded surface quality was evaluated. Specimens that were prepared by EDG with different machining parameters were analysed. With the aid of the morphological findings, different PCD erosion mechanisms were discussed. A comprehensive discussion was undertaken and the theoretical modelling of the process was obtained. The structural differences between PCD manufactured with EDG and conventional grinding were also compared. The performance test was conducted at the end of the methodology as a process evaluation.

Overall, the research seeks to better understand the PCD surface thermal damage caused by the EDG plasma and its influence on tool life. With this fundamental understanding, better process optimization and better PCD tools utilization can be expected.

Chapter 2 Literature Review

2.1. Introduction

The applications of PCD tools include the shaping of various materials, such as aluminium alloy used in the automotive industries, and wood, rock and rubber [1, 3, 10-13]. Due to PCD's excellent properties, this tool material is also regarded as the best candidate for machining exotic materials for the aerospace industries [14]. The significant hardness and excellent thermal conductivity of PCD, of up to 920 W/mK, makes it the most promising tool material for machining titanium [5]. In addition, several studies demonstrate the use of PCD in micro-machining glass and other micro optical-related devices made from tungsten carbide, electro-less plated nickel and silicon [15, 16]. In Printed Circuit Board (PCB) industries, PCD has also been used in the cutting tools with special blade configurations [2].

However, the outstanding mechanical, electrical and thermal properties of this material have a negative influence in that uneconomical and inefficient manufacturing processes often result [17, 18]. Low G ratios, high cutting force and high wheel cost pose the main challenges to conventional grinding production of PCD parts [17]. Similarly, for lapping processes, low efficiency, low removal rate, high cost and poor consistency are the major problems [17, 19, 20]. Experiments show that the G-ratio of conventional grinding of PCD tools is between 0.015 and 0.025 and MRR is between $0.226\text{mm}^3/\text{min}$ and $0.886\text{mm}^3/\text{min}$, depending on different grind size and structures [21]. Another problem with conventional grinding is the possibility of micro-cracks due to the high cutting force [21].

Brecher et al. [22] and Wang [23] used laser ablation, and achieved equivalent surface quality as abrasive grinding. However, unless ultra-short laser pulses of picoseconds were applied, which would result in unacceptably low MRR, a

conventional abrasive grinding process has to be followed in order to remove the severe heat affected zone [22]. In 2013, Qinjian et al. [24] developed another type of hybrid method by combining electrical discharge machining and ultrasonic-assisted mechanical grinding, but it was found that the hybrid method had limited impact on MRR. Likewise, Iwai et al. [25] developed an abrasive grinding-assisted EDM by using a metal-bounded diamond wheel for machining EC-PCD, but no obvious improvement in the grinding ratio was achieved in grinding conventional PCD material. For these reasons the EDM process is considered a good alternative for machining PCD due to its non-contact nature.

EDM is a non-conventional material removal process that uses thermal energy to melt or vaporize the work piece using high temperature sparks between the work piece and an electrode. EDM can be used for all conductive materials, regardless of their hardness and other mechanical properties, and is particularly good for fragile work pieces [26]. This chapter reviews the current achievements and findings of the EDM process of PCD.

2.2. PCD EDM Process

Early attempts to machine the diamond by EDM began in 1960. Heerschap et al. [27] revealed that non-conductive diamond could be machined using EDM by implementing a graphite coating on the diamond work piece. This is similar to the concept of “assisted electrode” used on EDM of insulated ceramics [28, 29]. To form the conductive coating of graphite, the diamond was heated up by non-oxidising flame to a temperature higher than its graphitization temperature [27, 30]. This was to ensure the conversion of diamond into graphite specifically on the work piece surface in order to provide a conductor path for spark initiation. The conductivity of the graphite enabled initial sparking and the erosion process was caused to the diamond-graphite conversion so that the process is self-sustaining. Hence, newly formed graphite was obtained on the eroded surface, providing connection to the current source [27, 30]. Figure 7 illustrates the aforementioned erosion concept.

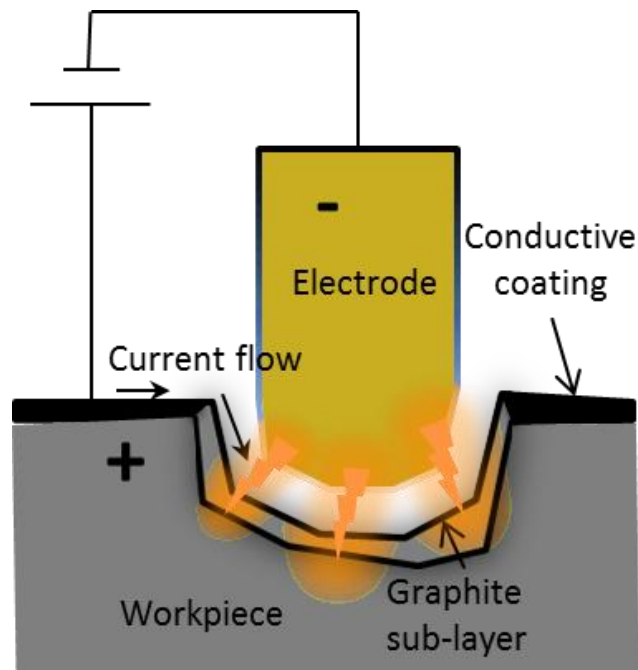


Figure 7: Graphite Coating Method

The emergence of PCD resolved the issues of non-conductivity of diamond. The presence of up to 15% by weight of metallic cobalt in the PCD composition makes it possible to machine PCD using EDM [6, 31-33]. Research on PCD EDM may be divided into Die/Sink EDM, EDG and Electrical Discharge Wire Machining (EDWM). Although they posit the same concept, EDG and EDWM vary significantly in machining parameters. Instead of static electrodes typically used in Die/Sink EDM, a rotating electrode wheel is used in EDG. This improves the flushing efficiency, since the rotating wheel electrode effectively drags dielectric into the gap. It thus yields better in-material removal rate, tool wear ratio and surface roughness [34-37].

2.2.1. EDM Polarity

Several studies show that a lesser electrode wear ratio was obtained when positive polarity of the tool electrode was used during EDM of PCD [6, 38]. Carbon plating of the positive electrode (which is the electrode in this case) was believed to be the reason for the reduction of electrode wear when this method is used [6, 39]. The

transformation of diamond into other forms of carbon occurs during the EDM sparking process. The result from the conversion process is the formation carbon ions, which are then involved in the positive electrode plating operation. This heat-resolved carbon acts as a shield that protects the electrode from wear [6]. Furthermore, the deposited carbon is also reported to come from the dielectric medium when hydrocarbon dielectric was used [40].

However, the adhesion also had a negative impact on process precision. Wang et al. [6] revealed that the formation of carbon adhesion (graphite and amorphous carbon) on the silver-tungsten alloy electrode rod led to increases in the effective electrode size. It thus produced a hole with a size bigger than the required dimension. Particularly in micro-hole machining, increase in the electrode size due to plating phenomena will significantly affect process precision. The comparison of the shape of electrodes after EDM with different polarity is shown in Figure 8.

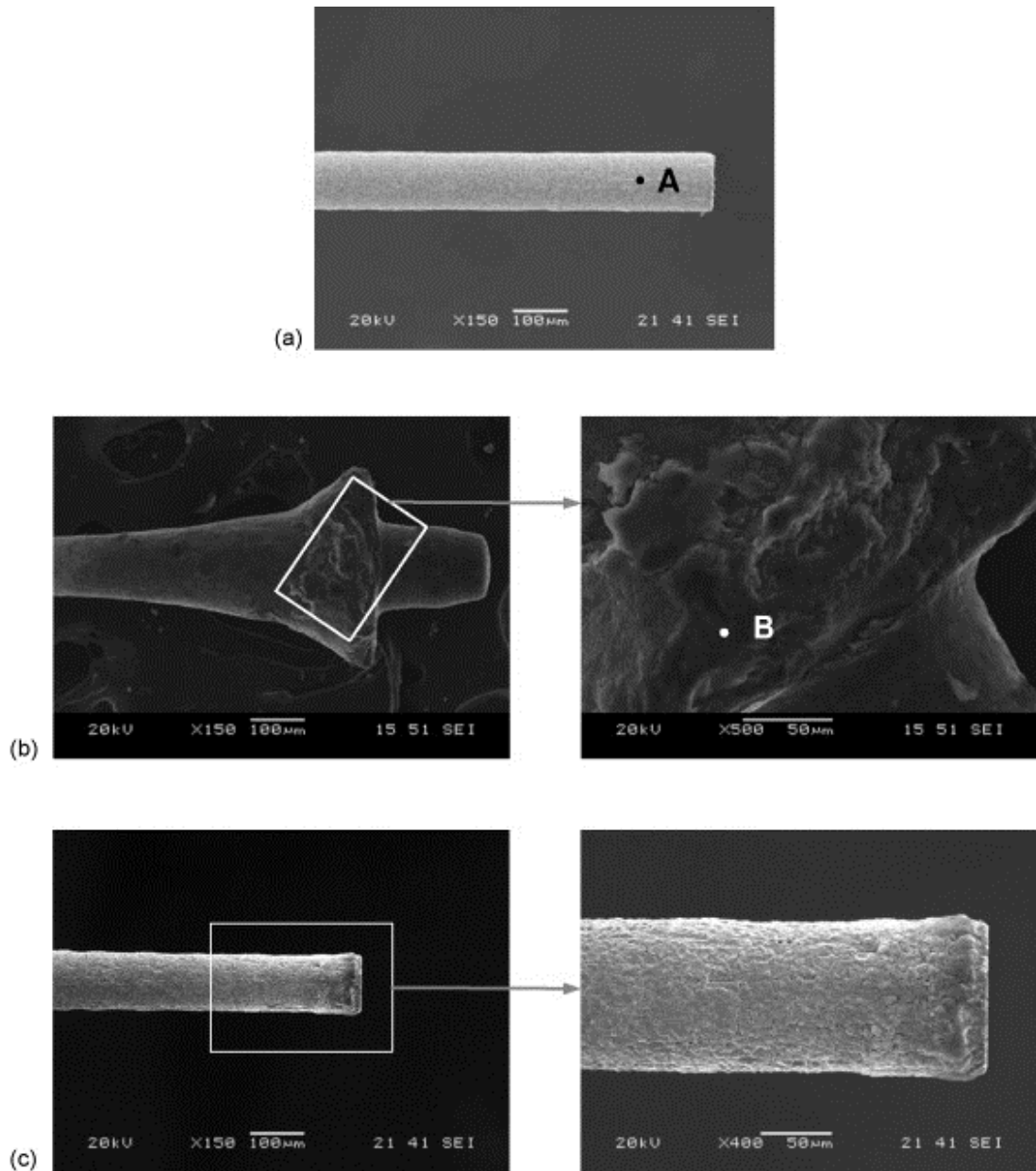


Figure 8: Comparison of electrode shape obtained by SEM after different polarity machining. (a) Initial shape of electrode (before machining) (b) Electrode after the positive polarity erosion (positive polarity of the tool electrode) (c) Electrode shape after negative polarity erosion (negative polarity of the tool electrode)[6]

2.2.2. Material Removal Rate

Considering the thermal conductivity, specific heat, and melting point of materials, Wang et al. [6] quantified the degree of difficulty for EDM of several materials. The degree of difficulty for a material to be eroded can be calculated using the following formula:

$$C_m = KCT_m^2 \quad (2.1)$$

where C_m is the erosion resistance index (ERI) ($10^{12} \text{ J} / \text{m s kg}$) and K , C and T_m are the thermal conductivity expressed in $\text{W}/(\text{mK})$, specific heat is expressed in $\text{J}/(\text{kg K})$, and melting point is expressed in K , respectively. As shown in Table 1, in comparison to the ERI of tungsten, copper and steel, the highest ERI was attributed to PCD, indicating that PCD is the hardest material to be eroded by EDM.

Table 1: Erosion resistance index (ERI) of materials [6]

Material	Erosion resistance index ($10^{12} \text{ J} / \text{m s kg}$)
Tungsten	2.99
Copper	2.79
Steel	0.230
PCD	4

It is well understood that the smaller PCD grain size will give better MRR, because it has higher electrical conductivity than PCD with bigger grains. This is due to the fact that PCD with smaller grain size has a higher proportion of cobalt content than is the case with bigger grain size PCD. Since cobalt is a highly conductive material and diamond is non-conductive, the electrical conductivity of smaller grain PCD is higher.

Figure 9 shows several strategies that have been applied to optimize the production rate in EDM machining of ordinary materials [41-45]. But, to the authors' knowledge, very little research has been reported on the effect of tool electrode material and dielectric in EDM machining of PCD. Current research for the purpose of improving the MRR in EDM of PCD is more focussed on the optimization of parameters. PCD is a highly thermally conductive material (a range of 250 to 920 W/mK) [5]. As a result, it suffers high energy losses per unit volume, which slows down the melting operation. Therefore, in a roughing operation, higher voltage and current are required to get the higher sparking energy for better MRR. However, it was reported that there is an interaction between the sparking energy and the charging process of capacitors. After a certain limit, charging capacitors of the EDM machine more than is required also results in lower MRR. Although higher energy is provided, a major amount of time was spent on the charging process [46].

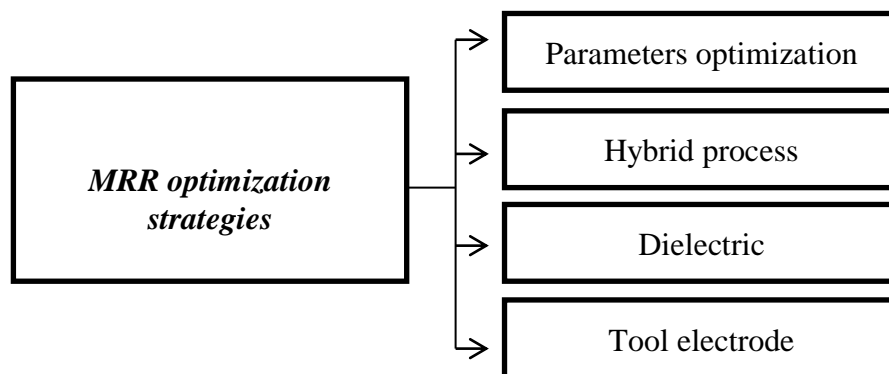


Figure 9: MRR optimization strategies

Parameter control is also important for avoiding a short circuit during the operation. Using the current and voltage feedback system integrated to the machine, a specific pulse known as normal, arc and short circuit pulses could be observed. Short circuit pulses occur when the electrode is in contact with the work piece and are believed not to contribute anything to removing material. However, the control activity of PCD EDM parameter is challenging, since the feedback system is not necessarily accurate in representing the real machining behaviour. As was found by Ye et al. [47], in some cases the short circuit pulses did not happen, although the electrode was contacting the PCD surface. This was due to the electrode making contact with a

non-conductive diamond particle that protruded from the PCD surface and the sparking still being between the cobalt and the electrode.

2.2.3. Surface Roughness and Morphology

Surface roughness is an important factor that affects the performance of cutting tools, particularly in high precision machining [5, 48]. Due to the extremely high hardness of PCD, together with high chemical stability, mechanical processing does not appear to be the best machining strategy for producing a very fine surface while considering the production cost [5].

In the roughing operation of PCD EDM, granularity of the surface results when individual diamond grains drop out of the surface, which makes the roughness value proportional to the grain size [1]. Hence, finer grain size is to be preferred when a better surface finish is a priority. However, in some tool applications, specifically in machining metal matrix composite (MMC) materials, bigger grain PCD is preferential. The investigation into the performance of PCD tools in machining of MMCs showed that better tool wear performance was achieved by PCD with bigger grains [49-51]. Although better in surface finish, a high percentage of cobalt in small PCD grain structure is also believed to be involved in weakening the structure, due to its affinity for carbon and its catalytic action in changing diamond to other forms of carbon at high temperatures [52]. For this reason, the investigation of surface roughness obtained by the fabrication process, especially for big PCD grain (10 μ m grain size and above), is crucial for the development of high performance tools.

Olsen et al. [32] believed that, during the sparking process, some diamond grains were lost as a result of the highly conductive cobalt network being preferentially eroded [31, 32]. For this reason, sparked PCD surfaces were generally of lower quality than conductive Chemical Vaporized Deposition (CVD) diamond film, so-called CVDITE CDE, even when fine diamond is used (2 μ m) [31]. Unlike PCD, in CVDITE CDE film production, the conductivity of diamond grains is increased by increasing the electrical conductivity of the diamond crystal itself through boron

doping [32]. Therefore, the spark will not only initiate on the grain boundary but can also happen on the grain surface. This led to the EDM of CVDITE CDE process cutting through the diamond crystal and not detaching the grains as a reason for finer surface value. [31]. To better understand the difference in mechanism, PCD and CVDITE CDE film material are compared in Table 2. It was believed that the major factor causing selective erosion of the PCD is the low electrical conductivity of diamond in contrast to the highly conductive cobalt path at the grain boundaries.

Table 2: Comparison between PCD and CVDITE CDE material

	PCD material	Conductive CVD (CVDITE CDE) material
Thermal conductivity	Around 459 W/mK (for 10 μ m grains)[53]	Up to 2200 W/mK[32]
Compositions	Consists of cobalt binder and diamond grains	Consists of no metallic second phase [32]
Grains structure	Diamond might comprising both lamellar and fine grains, depends on the production method and starting materials [54].	Comprising only columnar/ lamellar diamond grains [32].
Specific resistance	$1.4 \times 10^{-4} \Omega\text{m}$ [53]	$0.4 \sim 1 \times 10^{-3} \Omega\text{m}$ [55]

This principle has also been proved by Suzuki et al. [53]. A new type of PCD was developed by following the same concept as conductive CVDITE CDE. The boron atoms were incorporated into the diamond lattice in order to increase electrical conductivity [32, 53]. As a result, better surface finish than the standard PCD was achieved after the WEDM process. Interestingly, observation on the new PCD developed showed that the grain was flattened by the electro-discharge process (Figure 10). Better oxidation resistance might also be the other factor contributing to the lower surface roughness of the boron-doped PCD while EDMed in water dielectric. By oxidation analysis of CVD (CVDITE CDE), it was shown that better oxidation resistance is obtained when the diamond is doped with boron [55].

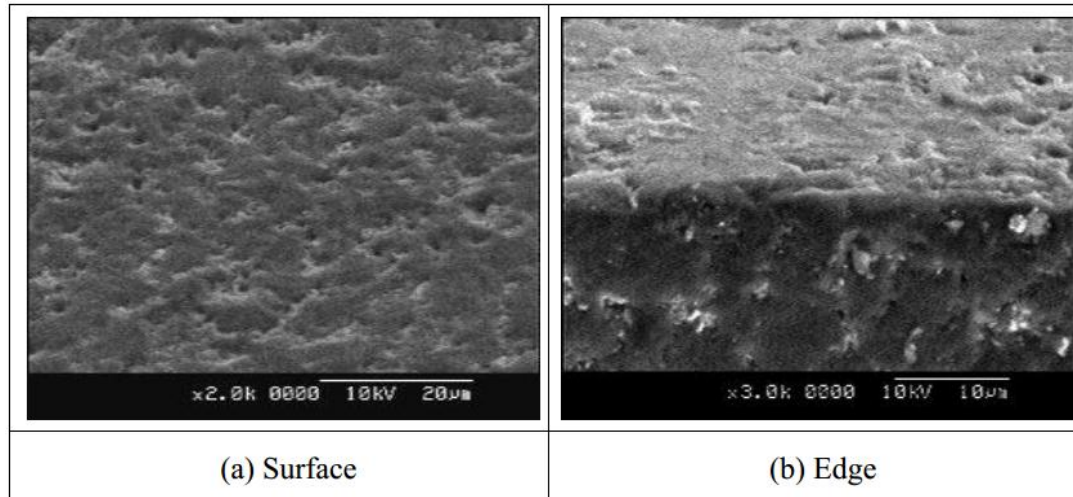


Figure 10:EDMed surfaces of boron doped PCD sample[53]

In the EDM process, discharge energy obtained by the spark significantly affects the roughness of the work piece surface. Although high sparking energy is desirable for better MRR, the higher the discharge energy, the higher the surface roughness will be [33]. Zhang et al. [56] claimed that low surface roughness obtained by low sparking energy is due to the chemical effect of molten cobalt. They believed that the temperature of the spark is high enough for diamond to graphite conversion on the surface. The converted diamond or graphite will then be dissolved into the molten cobalt before being removed easily by the blast that forms due to the dielectric oil vaporization [56]. The effect will not be significant when high sparking energy is used, since the cobalt will be vaporized [56].

In other study, even though with a similar sparking energy, Han et al. [57] believed that the surface roughness may not necessarily be similar. They stated that the heat flux generated from the process had a significant effect on the surface roughness as well as on surface morphology [57]. Heat flux, defined as the heat transfer rate per unit area, is related to the magnitude of current used during the EDM process. With the same sparking energy, the heat flux may not be the same. With the same discharge energy, a pulse with short duration and high peak current will give higher heat flux than a pulse with long duration and low peak current [57]. Consider the following basic formula for the temperature gradient calculation:

$$q = -K \Delta T \quad (2.2)$$

where ΔT , q and K are the temperature difference, heat flux and material conductivity, respectively. Rearrange equation 2.2 so that:

$$T_2 - T_1 = -q/K \quad (2.3)$$

Since the heat flux is a vectorial quantity, T_2 should be defined as the temperature on deeper surface and T_1 is the temperature of the surface that is exposed to the spark. Higher heat flux, defined as the higher heat rate per unit area, will reduce the chance of heat losses due to the conduction on the surface, thus creating deeper craters.

Little research has been done regarding the effect of dielectric in the machining of PCD materials. WEDM of PCD in oil can result in better surface quality than deionized water [53]. It was also reported that implementing WEDM of PCD in a water bath would increase the selective erosion on the cobalt region, since the cobalt has a much higher electrochemical equivalence than the other elements in PCD [58, 59]. Furthermore, the oxygen content in water also results in the oxidation of the PCD machined surface [55]. Wu et al. have shown the increase in oxygen content toward the edge of the WEDMed surface [59]. Figure 11 shows the voids that occurred due to the selective erosion of cobalt on the PCD surface.

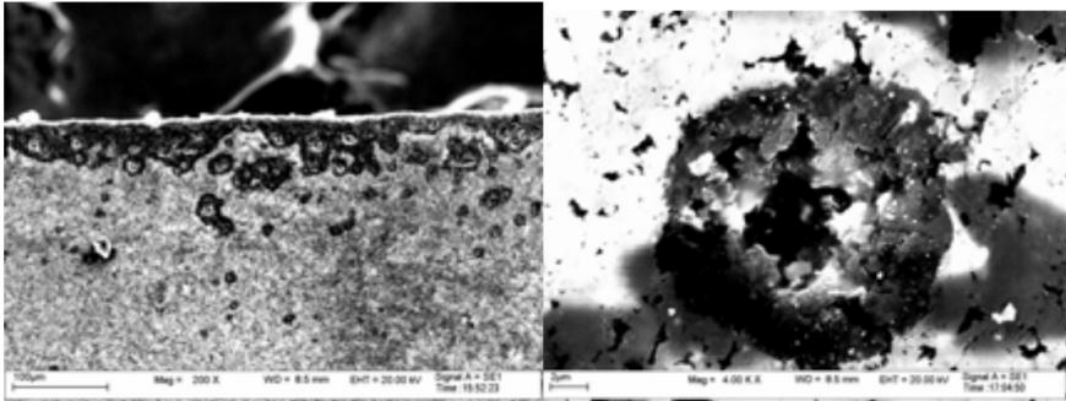


Figure 11: Void due to selective erosion [59]

2.2.4. Challenges on Cutting of Laminar Discs

The laminar disc blanks are made from PCD on a carbide substrate. Although the carbide substrate provides the PCD tools with sufficient toughness [60], EDM of this laminar structure is a challenge, since the layers are made of materials with dissimilar properties [58, 61]. Preferential erosion of the carbide occurs at the PCD-carbide interface and this not only causes a notch to form but also increases residual stress in this area [1]. The notch is believed to be more dominant when the bigger grain structure is used [1]. An analysis was conducted by Cao et al. [17] in an attempt to minimize the notch depth that was categorized as the most serious PCD surface defect caused by EDM. Through parameter optimization, they successfully reduced the notch depth on the diamond-WC interface to only 0.03mm [17].

Pisarciuc and Cristian [58] stated that “due to the manufacturing process, the cobalt concentration is higher in the transition zone between the carbide substrate and the diamond matrix. The low resistance of cobalt to thermal erosion compared with the other components, give rise to increased material removal in this area” [58]. This is proved by the element mapping result (Figure 12) obtained by Shin et al. [62] just after the HPHT sintering process of PCD. The result shows that the composition of cobalt is dominant on the PCD-WC interface. However, there is also an unexplained phenomenon which occurred during the roughing operation: formation of another notch that appeared just below the top edge of the PCD was observed [58]. Further study on the behaviour is needed to explain the phenomenon.

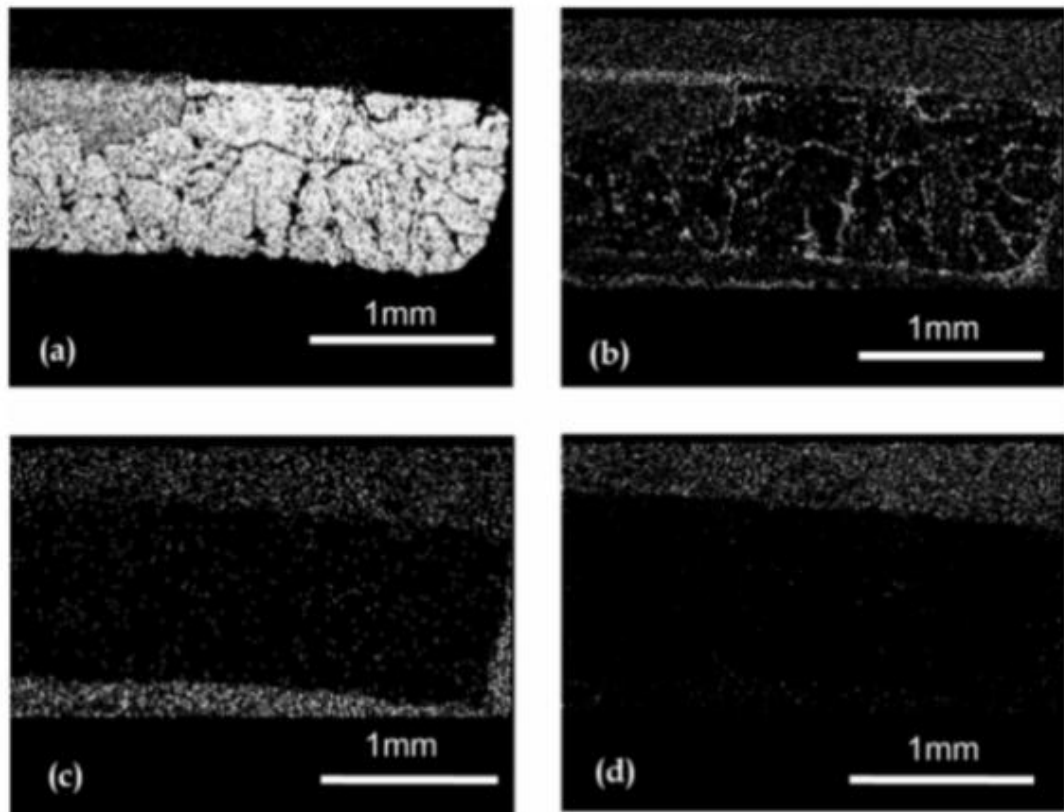


Figure 12: Element Mapping of (a) C, (b) Co, (c) Ta and (d) W [62]

2.2.5. Heat Affected Zone (HAZ)

In EDM of metals, the recast layer, also known as the white layer, is a thin layer on the surface of the work piece which is formed by the re-solidification of melted material that has not been swept away by the dielectric during the EDM process. This layer usually presents after the WEDM or Die Sinking EDM due to an inefficient flushing operation [58]. The melted material is quickly chilled, primarily by heat conditions in the bulk of the work piece, resulting in an exceedingly hard surface. For this reason, a smaller grained annealed microstructure is usually formed just beneath the machined surface which also results in better surface hardness [58, 63]. The surface integrity result from the EDM process on ordinary material (metals) is illustrated in Figure 13.

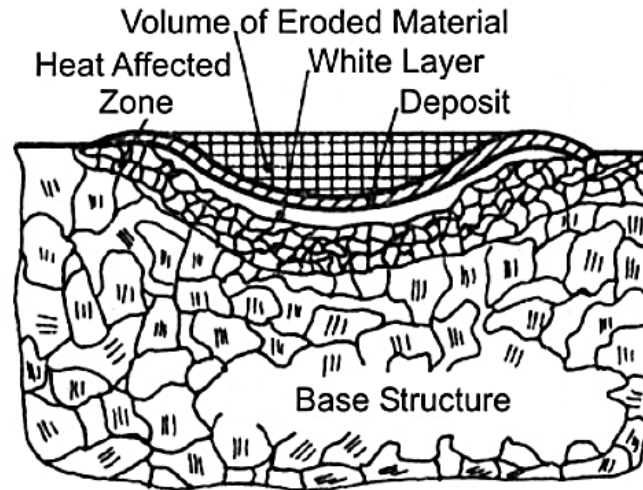


Figure 13: Heat affected zone of EDMed surface [58]

The heat affected zone (HAZ) when machining a metal is the zone that is subjected to very high temperatures, though not high enough to be melted, but which promotes some microstructure changes [43, 58, 64]. It will generally extend to a depth of a few microns beneath the machined surface. Research has shown that the surface damage due to the heat of plasma appeared up to 0.05mm in depth [31]. The depth is dependent on the temperature gradient profile, which is affected by the electrode materials, dielectric and machining conditions [43]. Although a recast layer may not be generated in the EDG of PCD, there will generally be a HAZ, which is largely unavoidable when dealing with thermal processing. This HAZ is also generally called the modified zone or affected layer by some researchers when dealing with PCD [65, 66].

Metallurgical examination of the surfaces using various techniques such as optical metallography, Scanning Electron Microscope (SEM), X-ray diffraction (XRD) and Raman spectroscopy has been undertaken by many researchers to study the behaviour of material due to thermal stress [65-77]. The affected layer with a thickness more than 70 μ m has been observed on the PCD surface after EDM with a roughing condition [65] (Figure 14a). The thickness of this layer is also believed to significantly affect PCD tool life. However, detailed explanation of the structural properties of this layer has remained unknown. As shown in Figure 14b, nearly the same layer was also observed by Kalyanasundram et al. on the PCD sample after

LWJ machining. Using the Raman analytical method, a laser that focused on the layer formed strongly indicates the formation of graphite. A high proportion of graphite on this area can be explained by the diamond to graphite conversion to be covered in section 2.2.6.

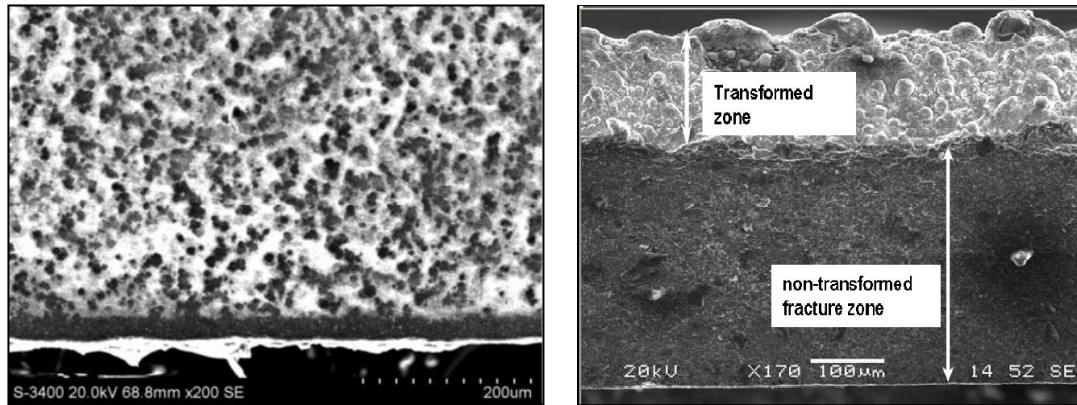


Figure 14: SEM image of PCD (a) after EDM (b) after LWJ [65, 66]

The failure of material structure usually starts from the surface [69]. Hence, in order to have better performance, the surface damage or defects should be controlled. Surface defects will induce stress concentration, leading to crack propagation [78]. Removing the damaged surface by grinding is not generally feasible, especially when a complex surface is involved. Surface cracking on EDMed PCD is typically associated with the heat generated by the process [1]. Increasing the heat will increase the PCD grain volume that will increase the residual stress especially on the surface. Once residual stress is increased over certain limits, initial cracks a few nanometres will be caused. These nano-scale cracks pose a major concern in making PCD cutting tools, because they are one of the main reasons for tool failure and short tool life. Rapid loading with machining vibration requires the tool to have high fatigue strength. Nano-cracks will tend to be propagated when the tool is under the fatigue loading. The crack will tend to appear on the grain boundary or diamond bridge (Figure 15), which is the weakest part of the microstructure. This causes dislodgement of diamond particles as the mechanism for tool wear [49].

References

- [1] T. B. Thoe, D. K. Aspinwall, M. L. H. Wise, and I. A. Oxley, "Polycrystalline diamond edge quality and surface integrity following electrical discharge grinding," *Journal of Materials Processing Technology*, vol. 56, pp. 773-785, 1996.
- [2] P.-L. Tso and Y.-G. Liu, "Study on PCD machining," *International Journal of Machine Tools and Manufacture*, vol. 42, pp. 331-334, 2002.
- [3] L. Jaworska, "Diamond-Ceramic Bonding Phase Composites for Application in Cutting Tools," *Ceramic Materials*, vol. 63, pp. 131-137, 2011.
- [4] J. Yan, Y. Murakami, and J. P. Davim, "Tool Design, Tool Wear and Tool Life," *Machining Dynamics*, pp. 117-149, 2009.
- [5] Y. Chen, L. C. Zhang, J. A. Arsecularatne, and C. Montross, "Polishing of polycrystalline diamond by the technique of dynamic friction, part 1: Prediction of the interface temperature rise," *International Journal of Machine Tools and Manufacture*, vol. 46, pp. 580-587, 2006.
- [6] D. Wang, W. S. Zhao, L. Gu, and X. M. Kang, "A study on micro-hole machining of polycrystalline diamond by micro-electrical discharge machining," *Journal of Materials Processing Technology*, vol. 211, pp. 3-11, 2011.
- [7] V. Schulze, C. Becke, K. Weidenmann, and S. Dietrich, "Machining strategies for hole making in composites with minimal workpiece damage by directing the process forces inwards," *Journal of Materials Processing Technology*, vol. 211, pp. 329-338, 2011.
- [8] R. M. Erasmus, J. D. Comins, V. Mofokeng, and Z. Martin, "Application of Raman spectroscopy to determine stress in polycrystalline diamond tools as a function of tool geometry and temperature," *Diamond and Related Materials*, vol. 20, pp. 907-911, 2011.
- [9] V. P. Astakhov and A. Stanley, "Polycrystalline Diamond (PCD) Tool Material: Emerging Applications, Problems, and Possible Solutions," in *Traditional Machining Processes*, ed: Springer, 2015, pp. 1-32.

- [10] M. H. Paul Harrison, Jozef Wendland, "Enhanced Cutting of Polycrystalline Diamond with a Q-switched Diode Pumped Solid State Laser," 2005.
- [11] Q. Bai, Y. Yao, and S. Chen, "Research and development of polycrystalline diamond woodworking tools," *International Journal of Refractory Metals and Hard Materials*, vol. 20, pp. 395-400, 2002.
- [12] P. J. Heath, "Developments in applications of PCD tooling," *Journal of Materials Processing Technology*, vol. 116, pp. 31-38, 2001.
- [13] V. Mărăscu-klein, "The application of carbon materials in advanced technologies."
- [14] J. Mo, S. L. Ding, A. Mackie, M. Brandt, S. J. Sun, R. Hoseinnezhad, and R. Webb, "Design of Exotic Materials Machining System," *Advanced Materials Research*, vol. 633, pp. 36-46, 2013.
- [15] T. Wada, T. Masaki, and D. W. Davis, "Development of micro grinding process using micro EDM trued diamond tools," in *ASPE Proceeding, Annual Meeting*, 2002, pp. 16-19.
- [16] C. J. Morgan, R. R. Vallance, and E. R. Marsh, "Micro machining glass with polycrystalline diamond tools shaped by micro electro discharge machining," *Journal of Micromechanics and Microengineering*, vol. 14, p. 1687, 2004.
- [17] F. Cao and Q. Zhang, "Neural network modelling and parameters optimization of increased explosive electrical discharge grinding (IEEDG) process for large area polycrystalline diamond," *Journal of Materials Processing Technology*, vol. 149, pp. 106-111, 2004.
- [18] G. F. Zhang, B. Zhang, Z. H. Deng, and J. F. Chen, "An Experimental Study on Laser Cutting Mechanisms of Polycrystalline Diamond Compacts," *CIRP Annals - Manufacturing Technology*, vol. 56, pp. 201-204, 2007.
- [19] M. Najafi-sani and P. A. Bex, "Shaping of bonded abrasive products," ed: EP Patent 0,368,654, 1994.
- [20] A. P. Malshe, B. S. Park, W. D. Brown, and H. A. Naseem, "A review of techniques for polishing and planarizing chemically vapor-deposited (CVD) diamond films and substrates," *Diamond and Related Materials*, vol. 8, pp. 1198-1213, 1999.

- [21] Y.-K. Liu and P.-L. Tso, "The optimal diamond wheels for grinding diamond tools," *The International Journal of Advanced Manufacturing Technology*, vol. 22, pp. 396-400, 2003.
- [22] C. Brecher, M. Emonts, J.-P. Hermani, and T. Storms, "Laser Roughing of PCD," *Physics Procedia*, vol. 56, pp. 1107-1114, 2014.
- [23] Q. Wu, J. Wang, and C. Huang, "Analysis of the machining performance and surface integrity in laser milling of polycrystalline diamonds," *Proceedings of the Institution of Mechanical Engineers, Part B: Journal of Engineering Manufacture*, vol. 228, pp. 903-917, 2014.
- [24] Z. Qinjian, Z. Luming, L. Jianyong, C. Yonglin, W. Heng, C. Yunan, S. Haikuo, Y. Xiaoqing, and L. Minzhi, "Study on electrical discharge and ultrasonic assisted mechanical combined machining of polycrystalline diamond," *Procedia CIRP*, vol. 6, pp. 589-593, 2013.
- [25] M. Iwai, S. Ninomiya, and K. Suzuki, "Effect of complex electrodischarge grinding for electrically conductive PCD," *Advanced Materials Research*, vol. 325, pp. 276-281, 2011.
- [26] K. Ho and S. Newman, "State of the art electrical discharge machining (EDM)," *International Journal of Machine Tools and Manufacture*, vol. 43, pp. 1287-1300, 2003.
- [27] C. M. Levitt, "Eroding of hard crystalline carbon," ed: Google Patents, 1960.
- [28] N. Mohri, Y. Fukuzawa, T. Tani, N. Saito, and K. Furutani, "Assisting electrode method for machining insulating ceramics," *CIRP Annals-Manufacturing Technology*, vol. 45, pp. 201-204, 1996.
- [29] T. Tani, Y. Fukuzawa, N. Mohri, N. Saito, and M. Okada, "Machining phenomena in WEDM of insulating ceramics," *Journal of Materials Processing Technology*, vol. 149, pp. 124-128, 2004.
- [30] M. Kunieda, B. Lauwers, K. P. Rajurkar, and B. M. Schumacher, "Advancing EDM through Fundamental Insight into the Process," *CIRP Annals - Manufacturing Technology*, vol. 54, pp. 64-87, 2005.
- [31] R. H. Olsen, D. K. Aspinwall, and R. C. Dewes, "Electrical discharge machining of conductive CVD diamond tool blanks," *Journal of Materials Processing Technology*, vol. 155-156, pp. 1227-1234, 2004.

- [32] R. H. Olsen, R. C. Dewes, and D. K. Aspinwall, "Machining of electrically conductive CVD diamond tool blanks using EDM," *Journal of Materials Processing Technology*, vol. 149, pp. 627-632, 2004.
- [33] J. M. Chris, R. R. Vallance, and R. M. Eric, "Micro machining glass with polycrystalline diamond tools shaped by micro electro discharge machining," *Journal of Micromechanics and Microengineering*, vol. 14, p. 1687, 2004.
- [34] S. S. Anand Pandey, "Current research trends in variants of Electrical Discharge Machining: A review," *International Journal of Engineering Science and Technology*, vol. Vol. 2(6), pp. 2172-2191, 2010.
- [35] J. S. Soni, "Microanalysis of debris formed during rotary EDM of titanium alloy (Ti 6Al 4V) and die steel (T 215 Cr12)," *Wear*, vol. 177, pp. 71-79, 1994.
- [36] P. Koshy, V. K. Jain, and G. K. Lal, "Experimental investigations into electrical discharge machining with a rotating disk electrode," *Precision Engineering*, vol. 15, pp. 6-15, 1993.
- [37] S. Singh and A. Bhardwaj, "Review to EDM by using water and powder-mixed dielectric fluid," *Journal of Minerals and Materials Characterization and Engineering*, vol. 10, p. 199, 2011.
- [38] E. Uhlmann and M. Roehner, "Investigations on reduction of tool electrode wear in micro-EDM using novel electrode materials," *CIRP Journal of Manufacturing Science and Technology*, vol. 1, pp. 92-96, 2008.
- [39] R. J. Weetnam, "The Characteristic of DC Arcd As Related to Electrical Discharge Machining," Department of Mechanical Engineering, Massachusetts Institute of Technology, 1968.
- [40] D. A. Khan and M. HAMEEDULLAH, "Effect of tool polarity on the Machining Characteristics in Electric Discharge Machining of Silver Steel and Statistical Modelling of the Process," *International Journal of Engineering Science*, vol. 3, 2011.
- [41] H. Zarepour, A. F. Tehrani, D. Karimi, and S. Amini, "Statistical analysis on electrode wear in EDM of tool steel DIN 1.2714 used in forging dies," *Journal of Materials Processing Technology*, vol. 187, pp. 711-714, 2007.

- [42] M. Jeswani, "Effect of the addition of graphite powder to kerosene used as the dielectric fluid in electrical discharge machining," *Wear*, vol. 70, pp. 133-139, 1981.
- [43] K. M. Shu and G. C. Tu, "Study of electrical discharge grinding using metal matrix composite electrodes," *International Journal of Machine Tools and Manufacture*, vol. 43, pp. 845-854, 2003.
- [44] S. Singh, S. Maheshwari, and P. Pandey, "Some investigations into the electric discharge machining of hardened tool steel using different electrode materials," *Journal of Materials Processing Technology*, vol. 149, pp. 272-277, 2004.
- [45] V. K. Meena, "Optimization of EDM machining parameters using DMLS electrode," *Rapid Prototyping Journal*, vol. 12, pp. 222-228, 2006.
- [46] S. Kumar, R. Singh, T. P. Singh, and B. L. Sethi, "Surface modification by electrical discharge machining: A review," *Journal of Materials Processing Technology*, vol. 209, pp. 3675-3687, 2009.
- [47] S. L. Ye, W. C. Pan, S. L. Ding, J. Mo, M. Brandt, and A. Mackie, "Electrical Discharge Characteristics of Polycrystalline Diamonds," *Advanced Materials Research*, vol. 426, pp. 44-47, 2012.
- [48] B. Podgornik, S. Hogmark, and O. Sandberg, "Influence of surface roughness and coating type on the galling properties of coated forming tool steel," *Surface and Coatings Technology*, vol. 184, pp. 338-348, 2004.
- [49] J. A. Arsecularatne, L. C. Zhang, and C. Montross, "Wear and tool life of tungsten carbide, PCBN and PCD cutting tools," *International Journal of Machine Tools and Manufacture*, vol. 46, pp. 482-491, 2006.
- [50] K. Weinert and W. König, "A Consideration of Tool Wear Mechanism when Machining Metal Matrix Composites (MMC)," *CIRP Annals - Manufacturing Technology*, vol. 42, pp. 95-98, 1993.
- [51] R. T. Coelho, S. Yamada, D. K. Aspinwall, and M. L. H. Wise, "The application of polycrystalline diamond (PCD) tool materials when drilling and reaming aluminium based alloys including MMC," *International Journal of Machine Tools and Manufacture*, vol. 35, pp. 761-774, 5// 1995.

- [52] F. A. Almeida, A. J. S. Fernandes, F. J. Oliveira, and R. F. Silva, "Semi-orthogonal turning of hardmetal with CVD diamond and PCD inserts at different cutting angles," *Vacuum*, vol. 83, pp. 1218-1223, 2009.
- [53] K. Suzuki, Y. Shiraishi, N. Nakajima, M. Iwai, S. Ninomiya, Y. Tanaka, and T. Uematsu, "Development of new PCD made up of boron doped diamond particles and its machinability by EDM," *Advanced Materials Research*, vol. 76, pp. 684-689, 2009.
- [54] T. I. Hitoshi SUMIYA, "Microstructure and Mechanical Properties of High-Hardness Nano-Polycrystalline Diamonds," *SEI Technical Review* pp. 85-91, April 2008 2008
- [55] A. Sharma, M. Iwai, K. Suzuki, and T. Uematsu, "Potential of electrically conductive chemical vapor deposited diamond as an electrode for micro-electrical discharge machining in oil and water," *New Diamond and Frontier Carbon Technology*, vol. 15, pp. 181-194, 2005.
- [56] Z. Zhang, H. Peng, and J. Yan, "Micro-cutting characteristics of EDM fabricated high-precision polycrystalline diamond tools," *International Journal of Machine Tools and Manufacture*, vol. 65, pp. 99-106, 2013.
- [57] F. Han, J. Jiang, and D. Yu, "Influence of discharge current on machined surfaces by thermo-analysis in finish cut of WEDM," *International Journal of Machine Tools and Manufacture*, vol. 47, pp. 1187-1196, 2007.
- [58] C. Pisarciuc, "Structure, Material Properties and Applications of Diamond-like Materials " *Nonconventional Technologies Review* pp. 13-18, 2012.
- [59] H. Wu, S. Kanno, K. Liu, S. Ng, W. Fong, and D. Pan, "Development of polycrystalline diamond cutting tool fabrication technology," *Parameters*, vol. 1, p. 3.
- [60] V. P. Astakhov and J. P. Davim, "Tools (geometry and material) and tool wear," *Machining. Fundamentals and Recent Advances*, pp. 37-52, 2008.
- [61] K. Bertagnolli and R. Vale, "Understanding and controlling residual stresses in thick polycrystalline diamond cutters for enhanced durability," *Finer Points(USA)*, vol. 12, p. 20, 2000.
- [62] T. J. Shin, J. O. Oh, K. Hwan Oh, and D. N. Lee, "The mechanism of abnormal grain growth in polycrystalline diamond during high pressure-high

- temperature sintering," *Diamond and Related Materials*, vol. 13, pp. 488-494, 2004.
- [63] S. K. Hargrove and D. Ding, "Determining cutting parameters in wire EDM based on workpiece surface temperature distribution," *The International Journal of Advanced Manufacturing Technology*, vol. 34, pp. 295-299, 2007.
- [64] O. E. Buğlent Ekmekci, A. Erman Tekkaya, Abdulkadir Erden, "Residual stress state and hardness depth in electric discharge machining: De-ionized water as dielectric liquid," *Machine Science and Technology*, vol. 9, pp. 39-61, 2005.
- [65] Y. H. Jia, J. G. Li, and X. J. Lu, "Study on EDM Machining Technics of Polycrystalline Diamond Cutting Tool and PCD Cutting Tool's Life," *Advanced Materials Research*, vol. 268, pp. 309-315, 2011.
- [66] D. Kalyanasundaram, A. Schmidt, P. Shrotriya, and P. Molian, "Understanding thermo-chemical machining of polycrystalline diamond by hybrid laser/waterjet system," *Mechanics guided design of hybrid laser/waterjet system for machining of hard and brittle materials*, p. 97, 2009.
- [67] V. Yadav, V. K. Jain, and P. M. Dixit, "Thermal stresses due to electrical discharge machining," *International Journal of Machine Tools and Manufacture*, vol. 42, pp. 877-888, 2002.
- [68] S. A. Catledge, Y. K. Vohra, R. Ladi, and G. Rai, "Micro-Raman stress investigations and X-ray diffraction analysis of polycrystalline diamond (PCD) tools," *Diamond and Related Materials*, vol. 5, pp. 1159-1165, 1996.
- [69] H. K. a. T. S. Yoshiaki Akiniwa, "Effect of Residual stresses on Fatigue Strength of Severely Surface Deformed Steels by Shot Peening," *JCPDS-International Centre for Diffraction Data*, pp. 493-500, 2009.
- [70] R. R. d. A. Bojan Marinkovica*, Alvaro Saavedrab, Fernando Cosme Rizzo Assunçãoa, "A Comparison between the Warren-Averbach Method and Alternate Methods for X-Ray Diffraction Microstructure Analysis of Polycrystalline Specimens," *Materials Research*, vol. Vol. 4, pp. 71-76, 2001.
- [71] D. A. Lucca, E. Brinksmeier, and G. Goch, "Progress in Assessing Surface and Subsurface Integrity," *CIRP Annals - Manufacturing Technology*, vol. 47, pp. 669-693, 1998.

- [72] A. Heiman, E. Lakin, E. Zolotoyabko, and A. Hoffman, "Microstructure and stress in nano-crystalline diamond films deposited by DC glow discharge CVD," *Diamond and Related Materials*, vol. 11, pp. 601-607, 2002.
- [73] N. G. Ferreira, E. Abramof, E. J. Corat, N. F. Leite, and V. J. Trava-Airoldi, "Stress study of HFCVD boron-doped diamond films by X-ray diffraction measurements," *Diamond and Related Materials*, vol. 10, pp. 750-754, 2001.
- [74] Z. Nibennaoune, D. George, F. Antoni, S. Ahzi, D. Ruch, J. Gracio, and Y. Remond, "Corrigendum to "Improving diamond coating on Ti6Al4V substrate using a diamond like carbon interlayer: Raman residual stress evaluation and AFM analyses" [Diam. Relat. Mater. February 22 2012, 105-112]," *Diamond and Related Materials*, vol. 31, p. 81, 2013.
- [75] S. Chowdhury, M. T. Laugier, and J. Henry, "XRD stress analysis of CVD diamond coatings on SiC substrates," *International Journal of Refractory Metals and Hard Materials*, vol. 25, pp. 39-45, 2007.
- [76] P. Goudeau, L. Vandenbulcke, C. Met, M. I. De Barros, P. Andreazza, D. Thiaudiere, and M. Gailhanou, "X-ray diffraction analysis of residual stresses in smooth fined-grain diamond coatings deposited on TA6V alloys," *Surface and Coatings Technology*, vol. 200, pp. 170-173, 2005.
- [77] Y. Kang, Y. Qiu, Z. Lei, and M. Hu, "An application of Raman spectroscopy on the measurement of residual stress in porous silicon," *Optics and Lasers in Engineering*, vol. 43, pp. 847-855, 2005.
- [78] E. O. Ezugwu, J. Bonney, R. B. Da Silva, and O. Cakir, "Surface integrity of finished turned Ti-6Al-4V alloy with PCD tools using conventional and high pressure coolant supplies," *International Journal of Machine Tools and Manufacture*, vol. 47, pp. 884-891, 2007.
- [79] T. H. C. Childs, D. Dornfeld, S. Min, K. Sekiya, R. Tezuka, and Y. Yamane, "The influence of cutting edge sharpness on surface finish in facing with round nosed cutting tools," ed, 2008.
- [80] A. Ogiev and K. Chou, "Cutting Edge Profile Characterizations by White-Light Interferometry," in *2009 ASME Early Career Technical Conference*, 2009, pp. 19.1-19.8.
- [81] G. Oosthuizen, G. Akdogan, and N. Treurnicht, "The performance of PCD tools in high-speed milling of Ti6Al4V," *The International Journal of*

- Advanced Manufacturing Technology*, vol. 52, pp. 929-935, 2011/02/01 2011.
- [82] X. Zhang, C. Nath, A. S. Kumar, M. Rahman, and K. Liu, "A Study on Ultrasonic Elliptical Vibration Cutting of Hardened Steel Using PCD Tools," *ASME Conference Proceedings*, vol. 2010, pp. 163-169, 2010.
- [83] Y. Chen, L. C. Zhang, and J. A. Arsecularatne, "Polishing of polycrystalline diamond by the technique of dynamic friction. Part 2: Material removal mechanism," *International Journal of Machine Tools and Manufacture*, vol. 47, pp. 1615-1624, 2007.
- [84] P. Withers and H. Bhadeshia, "Residual stress. Part 1—measurement techniques," *Materials Science and Technology*, vol. 17, pp. 355-365, 2001.
- [85] N. Bondarenko, I. Petrusha, and V. Mechnik, "Drill bits with thermostable PCD inserts."
- [86] J. Kozak, K. Rajurkar, and S. Wang, "Material removal in WEDM of PCD blanks," *Journal of Engineering for Industry*, vol. 116, pp. 363-369, 1994.
- [87] F. L. Amorim, W. L. Weingaertner, and I. A. Bassani, "Aspects on the optimization of die-sinking EDM of tungsten carbide-cobalt," *Journal of the Brazilian Society of Mechanical Sciences and Engineering*, vol. 32, pp. 496-502, 2010.
- [88] C. Pisarciuc, "Machining Depth and Energy Consumption at Electrical Discharge Machining Of Polycrystalline Diamond," *Nonconventional Technologies Review*, vol. 18, pp. 78-82, 2014.
- [89] J. Filik, "Raman spectroscopy: a simple, non-destructive way to characterise diamond and diamond-like materials," *Spectroscopy Europe*, vol. 17, p. 10, 2005.
- [90] R. Shroder, R. Nemanich, and J. Glass, "Analysis of the composite structures in diamond thin films by Raman spectroscopy," *Physical review B*, vol. 41, p. 3738, 1990.
- [91] F. Tuinstra and J. L. Koenig, "Raman spectrum of graphite," *The Journal of Chemical Physics*, vol. 53, p. 1126, 1970.
- [92] N. Wada and S. Solin, "Raman efficiency measurements of graphite," *Physica B+ C*, vol. 105, pp. 353-356, 1981.

- [93] P. S. Prevey, "X-ray diffraction residual stress techniques," *ASM International, ASM Handbook.*, vol. 10, pp. 380-392, 1986.
- [94] N. G. Ferreira, E. Abramof, E. J. Corat, and V. J. Trava-Airoldi, "Residual stresses and crystalline quality of heavily boron-doped diamond films analysed by micro-Raman spectroscopy and X-ray diffraction," *Carbon*, vol. 41, pp. 1301-1308, 2003.
- [95] G. Yingfei, X. Jiuhua, and Y. Hui, "Diamond tools wear and their applicability when ultra-precision turning of SiC_p/2009Al matrix composite," *Wear*, vol. 269, pp. 699-708, 2010.
- [96] J. O. Orwa, K. W. Nugent, D. N. Jamieson, and S. Praver, "Raman investigation of damage caused by deep ion implantation in diamond," *Physical Review B*, vol. 62, pp. 5461-5472, 09/01/ 2000.
- [97] N. Ferreira, E. Abramof, E. Corat, and V. Trava-Airoldi, "Residual stresses and crystalline quality of heavily boron-doped diamond films analysed by micro-Raman spectroscopy and X-ray diffraction," *Carbon*, vol. 41, pp. 1301-1308, 2003.
- [98] K. Suzuki, T. Saito, S. Sano, M. Iwai, S. Ninomiya, and T. Uematsu, "Manufacturing of a porous PCD with skeleton structure by EDM," *電気加工学会全国大会講演論文集*, vol. 2007, pp. 58-63, 2007.
- [99] S. Giménez, O. Van der Biest, and J. Vleugels, "The role of chemical wear in machining iron based materials by PCD and PCBN super-hard tool materials," *Diamond and related materials*, vol. 16, pp. 435-445, 2007.
- [100] M. Iwai, S. Sano, W. Pan, K. Itagaki, Y. Murakami, M. Wang, T. Uematsu, and K. Suzuki, "Manufacturing of micro V-groove with an electrically conductive diamond electrode in EDM," in *American Society for Precision Engineering 21st Annual Meeting*, Monterey, California, 2006.
- [101] Y. Chen, "Polishing of polycrystalline diamond composites," 2007.
- [102] M. Yoshikawa, Y. Mori, M. Maegawa, G. Katagiri, H. Ishida, and A. Ishitani, "Raman scattering from diamond particles," *Applied physics letters*, vol. 62, pp. 3114-3116, 1993.
- [103] C. Pisarciuc, "Study of Process Parameters at Electrical Discharge Machining of Polycrystalline Diamond," *Nonconventional Technologies Review*, pp. 54-58, 2013.

- [104] M. Zulafif Rahim, S. Ding, and J. Mo, "Electrical Discharge Grinding of Polycrystalline Diamond—Effect of Machining Parameters and Finishing In-Feed," *Journal of Manufacturing Science and Engineering*, vol. 137, pp. 021017-021017, 2015.
- [105] J. Y. Pei, C. N. Guo, and D. J. Hu, "Electrical discharge grinding of polycrystalline diamond," in *Materials Science Forum*, 2004, pp. 457-461.
- [106] P. Koshy, V. K. Jain, and G. K. Lal, "Grinding of cemented carbide with electrical spark assistance," *Journal of Materials Processing Technology*, vol. 72, pp. 61-68, 1997.
- [107] P. Koshy, V. K. Jain, and G. K. Lal, "Mechanism of material removal in electrical discharge diamond grinding," *International Journal of Machine Tools and Manufacture*, vol. 36, pp. 1173-1185, 1996.
- [108] P. Shankar, V. Jain, and T. Sundararajan, "Analysis of spark profiles during EDM process," *Machining science and technology*, vol. 1, pp. 195-217, 1997.
- [109] S. L. Ding, J. Mo, M. Brandt, and R. Webb, "Electric Discharge Grinding of Polycrystalline Diamond Materials," *Applied Mechanics and Materials*, vol. 271, pp. 333-337, 2013.
- [110] S. Katayama and M. Hashimura, "Effects of microcracks in CVD coating layers on cemented carbide and cermet substrates on residual stress and transverse rupture strength," *Journal of manufacturing science and engineering*, vol. 119, pp. 50-54, 1997.
- [111] M. Yahiaoui, L. Gerbaud, J. Y. Paris, J. Denape, and A. Dourfaye, "A study on PDC drill bits quality," *Wear*, vol. 298–299, pp. 32-41, 2013.
- [112] D. Che, P. Han, P. Guo, and K. Ehmann, "Issues in Polycrystalline Diamond Compact Cutter–Rock Interaction From a Metal Machining Point of View—Part II: Bit Performance and Rock Cutting Mechanics," *Journal of Manufacturing Science and Engineering*, vol. 134, p. 064002, 2012.
- [113] J. Paggett, E. Drake, A. Krawitz, R. Winholtz, and N. Griffin, "Residual stress and stress gradients in polycrystalline diamond compacts," *International Journal of Refractory Metals and Hard Materials*, vol. 20, pp. 187-194, 2002.

- [114] F. Chen, G. Xu, C.-d. Ma, and G.-p. Xu, "Thermal residual stress of polycrystalline diamond compacts," *Transactions of Nonferrous Metals Society of China*, vol. 20, pp. 227-232, 2010.
- [115] H. Jia, X. Jia, Y. Xu, L. Wan, K. Jie, and H. Ma, "Effects of initial crystal size of diamond powder on surface residual stress and morphology in polycrystalline diamond (PCD) layer," *Science China Physics, Mechanics and Astronomy*, vol. 54, pp. 98-101, 2011/01/01 2011.
- [116] A. Krawitz, R. Andrew Winholtz, E. Drake, and N. Griffin, "Residual stresses in polycrystalline diamond compacts," *International Journal of Refractory Metals and Hard Materials*, vol. 17, pp. 117-122, 1999.
- [117] R. H. Frushour, "Composite polycrystalline compact with improved fracture and delamination resistance," ed: Google Patents, 1996.
- [118] V. García Navas, I. Ferreres, J. A. Marañón, C. Garcia-Rosales, and J. Gil Sevillano, "Electro-discharge machining (EDM) versus hard turning and grinding—Comparison of residual stresses and surface integrity generated in AISI O1 tool steel," *Journal of Materials Processing Technology*, vol. 195, pp. 186-194, 2008.
- [119] Y. H. Guu and H. Hocheng, "Improvement of fatigue life of electrical discharge machined AISI D2 tool steel by TiN coating," *Materials Science and Engineering: A*, vol. 318, pp. 155-162, 2001.
- [120] Y. H. Guu, H. Hocheng, C. Y. Chou, and C. S. Deng, "Effect of electrical discharge machining on surface characteristics and machining damage of AISI D2 tool steel," *Materials Science and Engineering: A*, vol. 358, pp. 37-43, 2003.
- [121] H. T. Lee, T. Y. Tai, C. Liu, F. C. Hsu, and J. M. Hsu, "Effect of Material Physical Properties on Residual Stress Measurement by EDM Hole-Drilling Method," *Journal of Engineering Materials and Technology*, vol. 133, pp. 021014-021014, 2011.
- [122] J. Kozak, K. P. Rajurkar, and S. Z. Wang, "Material Removal in WEDM of PCD Blanks," *Journal of Manufacturing Science and Engineering*, vol. 116, pp. 363-369, 1994.
- [123] D. Che, P. Han, P. Guo, and K. Ehmann, "Issues in Polycrystalline Diamond Compact Cutter–Rock Interaction From a Metal Machining Point of View—

- Part I: Temperature, Stresses, and Forces," *Journal of Manufacturing Science and Engineering*, vol. 134, p. 064001, 2012.
- [124] M. Cai, X. Li, and M. Rahman, "Study of the mechanism of groove wear of the diamond tool in nanoscale ductile mode cutting of monocrystalline silicon," *Journal of manufacturing science and engineering*, vol. 129, pp. 281-286, 2007.
- [125] S. Bhowmick and A. Alpas, "The Performance of Diamond-Like Carbon Coated Drills in Thermally Assisted Drilling of Ti-6Al-4V," *Journal of Manufacturing Science and Engineering*, vol. 135, p. 061019, 2013.
- [126] V. Andreev, "Spontaneous graphitization and thermal disintegration of diamond at $T > 2000$ K," *Physics of the Solid State*, vol. 41, pp. 627-632, 1999.
- [127] S. Praver, K. Nugent, D. Jamieson, J. Orwa, L. A. Bursill, and J. Peng, "The Raman spectrum of nanocrystalline diamond," *Chemical Physics Letters*, vol. 332, pp. 93-97, 2000.
- [128] M. Ali, M. Ürgen, and M. Atta, "Effect of surface treatment on hot-filament chemical vapour deposition grown diamond films," *Journal of Physics D: Applied Physics*, vol. 45, p. 045301, 2012.
- [129] J. Lewis, S. Gittard, R. Narayan, C. Berry, R. Brigmon, R. Ramamurti, and R. Singh, "Assessment of microbial biofilm growth on nanocrystalline diamond in a continuous perfusion environment," *Journal of manufacturing science and engineering*, vol. 132, p. 030919, 2010.
- [130] D. Ramanathan and P. A. Molian, "Micro-and sub-micromachining of type IIa single crystal diamond using a Ti: Sapphire femtosecond laser," *Journal of manufacturing science and engineering*, vol. 124, pp. 389-396, 2002.
- [131] K. Mlungwane, M. Herrmann, and I. Sigalas, "The low-pressure infiltration of diamond by silicon to form diamond–silicon carbide composites," *Journal of the European Ceramic Society*, vol. 28, pp. 321-326, 2008.
- [132] L. Li, Z. Zhu, Z. Yan, G. Lu, and L. Rintoul, "Catalytic ammonia decomposition over Ru/carbon catalysts: the importance of the structure of carbon support," *Applied Catalysis A: General*, vol. 320, pp. 166-172, 2007.
- [133] D. Kalyanasundaram, A. Schmidt, P. Molian, and P. Shrotriya, "Hybrid CO₂ Laser/Waterjet Machining of Polycrystalline Diamond Substrate: Material

- Separation Through Transformation Induced Controlled Fracture," *Journal of Manufacturing Science and Engineering*, vol. 136, pp. 041001-041001, 2014.
- [134] C. Johnston, A. Crossley, P. Chalker, I. Buckley-Golder, and K. Kobashi, "High temperature Raman studies of diamond thin films," *Diamond and Related Materials*, vol. 1, pp. 450-456, 1992.
- [135] M. Z. Rahim, A. Pourmoslemi, S. L. Ding, and J. Mo, "Residual Stress Analysis of Polycrystalline Diamond after Electrical Discharge Machining," *Advanced Materials Research*, vol. 820, pp. 106-109, 2013.
- [136] M. Z. Rahim, S. Ding, B. Hu, and J. Mo, "Crater size prediction in electrical discharge grinding (EDG) of polycrystalline diamond (PCD)," *Romania*, 2014.
- [137] J. Thewlis and A. Davey, "XL. Thermal expansion of diamond," *Philosophical Magazine*, vol. 1, pp. 409-414, 1956.
- [138] Z. Li, H. Jia, H. Ma, W. Guo, X. Liu, G. Huang, R. Li, and X. Jia, "FEM analysis on the effect of cobalt content on thermal residual stress in polycrystalline diamond compact (PDC)," *Science China Physics, Mechanics and Astronomy*, vol. 55, pp. 639-643, 2012.
- [139] K. Uehara and S. Yamaya, "High pressure sintering of diamond by cobalt infiltration," *Science and Technology of New Diamond*, Satio, S. et al., Eds., Tokyo: KTK Scientific Publishers/Terra Scientific Publishing Company (TERRAPUB), pp. 203-209, 1990.
- [140] T. Evans, S. Davey, and S. Robertson, "Photoluminescence studies of sintered diamond compacts," *Journal of materials science*, vol. 19, pp. 2405-2414, 1984.
- [141] J. Tao, J. Ni, and A. J. Shih, "Modeling of the anode crater formation in electrical discharge machining," *Journal of Manufacturing Science and Engineering*, vol. 134, p. 011002, 2012.
- [142] D. D. DiBitonto, P. T. Eubank, M. R. Patel, and M. A. Barrufet, "Theoretical models of the electrical discharge machining process. I. A simple cathode erosion model," *Journal of Applied Physics*, vol. 66, pp. 4095-4103, 1989.
- [143] M. R. Patel, M. A. Barrufet, P. T. Eubank, and D. D. DiBitonto, "Theoretical models of the electrical discharge machining process. II. The anode erosion model," *Journal of Applied Physics*, vol. 66, pp. 4104-4111, 1989.

- [144] J. Marafona and J. Chousal, "A finite element model of EDM based on the Joule effect," *International Journal of Machine Tools and Manufacture*, vol. 46, pp. 595-602, 2006.
- [145] S. V. Kidalov and F. M. Shakhov, "Thermal conductivity of diamond composites," *Materials*, vol. 2, pp. 2467-2495, 2009.
- [146] D. J. Weidner, Y. Wang, and M. T. Vaughan, "Strength of diamond," *Science*, vol. 266, pp. 419-422, 1994.
- [147] C. Dold, M. Henerichs, L. Bochmann, and K. Wegener, "Comparison of Ground and Laser Machined Polycrystalline Diamond (PCD) Tools in Cutting Carbon Fiber Reinforced Plastics (CFRP) for Aircraft Structures," *Procedia CIRP*, vol. 1, pp. 178-183, // 2012.
- [148] D. Ishimarua, M. Tougea, H. Muta, A. Kubota, T. Sakamoto, and S. Sakamoto, "Burr suppression using sharpened PCD cutting edge by ultraviolet-ray irradiation assisted polishing," *Procedia CIRP*, vol. 1, pp. 184-189, 2012.
- [149] R. Kuppuswamy, K.-A. Airey, and H. Sardikmen, "Micro-grinding characteristics of polycrystalline diamond tool," *The International Journal of Advanced Manufacturing Technology*, pp. 1-11, 2014.
- [150] C.-F. Wyen and K. Wegener, "Influence of cutting edge radius on cutting forces in machining titanium," *CIRP Annals-Manufacturing Technology*, vol. 59, pp. 93-96, 2010.
- [151] K. Liu, X. P. Li, M. Rahman, and X. D. Liu, "Study of ductile mode cutting in grooving of tungsten carbide with and without ultrasonic vibration assistance," *The International Journal of Advanced Manufacturing Technology*, vol. 24, pp. 389-394, 2004/09/01 2004.
- [152] W. Hintze, H. Frömming, and A. Dethlefs, "Influence of machining with defined cutting edge on the subsurface microstructure of WC-Co parts," *International Journal of Refractory Metals and Hard Materials*, vol. 28, pp. 274-279, 3// 2010.
- [153] K. Nakamoto, K. Katahira, H. Ohmori, K. Yamazaki, and T. Aoyama, "A study on the quality of micro-machined surfaces on tungsten carbide generated by PCD micro end-milling," *CIRP Annals - Manufacturing Technology*, vol. 61, pp. 567-570, // 2012.

- [154] K. Harano, T. Satoh, H. Sumiya, and S.-t. KUKINO, "Cutting performance of nano-polycrystalline diamond," *SEI Tech Rev*, vol. 77, pp. 98-103, 2010.
- [155] J. Field, "The mechanical and strength properties of diamond," *Reports on Progress in Physics*, vol. 75, p. 126505, 2012.
- [156] Y. Chen, L. C. Zhang, and F. Tang, "Surface integrity of PCD composites generated by dynamic friction polishing: Effect of processing conditions," *Diamond and Related Materials*, vol. 26, pp. 25-31, 2012.
- [157] Y. Chen and L. Zhang, "Quality Verification of Polished PCD Composites by Examining the Phase Transformations," in *IUTAM Symposium on Surface Effects in the Mechanics of Nanomaterials and Heterostructures*, 2013, pp. 147-156.
- [158] Y. Chen and L. C. Zhang, "Polishing of polycrystalline diamond by the technique of dynamic friction, part 4: Establishing the polishing map," *International Journal of Machine Tools and Manufacture*, vol. 49, pp. 309-314, 3// 2009.
- [159] A. Bordin, S. Bruschi, A. Ghiotti, and P. F. Bariani, "Analysis of tool wear in cryogenic machining of additive manufactured Ti6Al4V alloy," *Wear*, vol. 328–329, pp. 89-99, 4/15/ 2015.
- [160] J. Simao, H. Lee, D. Aspinwall, R. Dewes, and E. Aspinwall, "Workpiece surface modification using electrical discharge machining," *International Journal of Machine Tools and Manufacture*, vol. 43, pp. 121-128, 2003.
- [161] B. Jiang, S. Lan, J. Ni, and Z. Zhang, "Experimental investigation of spark generation in electrochemical discharge machining of non-conducting materials," *Journal of Materials Processing Technology*, vol. 214, pp. 892-898, 2014.